analytical chemistry

Technical Note

pubs.acs.org/ac

Biocompatible Microfabrication of 3D Isolation Chambers for Targeted Confinement of Individual Cells and Their Progeny

Jason C. Harper,[†,‡] Susan M. Brozik,[†,‡] C. Jeffrey Brinker,[†,‡] and Bryan Kaehr*[,†,‡]

[†]Sandia National Laboratories, Albuquerque, New Mexico 87131, United States

[‡]Department of Chemical and Nuclear Engineering, University of New Mexico, Albuquerque, New Mexico 87106, United States

Supporting Information

ABSTRACT: We describe a technique to physically isolate single/individual cells from their surrounding environment by fabricating three-dimensional microchambers around selected cells under biocompatible conditions. Isolation of targeted cells is achieved via rapid fabrication of protein hydrogels from a biocompatible precursor solution using multiphoton lithography, an intrinsically 3D laser direct write microfabrication technique. Cells remain chemically accessible to environmental cues enabling their propagation into well-defined, high density populations. We demonstrate this methodology on gram negative (*E. coli*), gram positive (*S. aureus*), and eukaryotic (*S. cerevisiae*) cells. The opportunities to confine viable, single/individual-cells and small populations within user-defined microenvironments afforded by this approach should facilitate the study of cell behaviors across multiple generations.

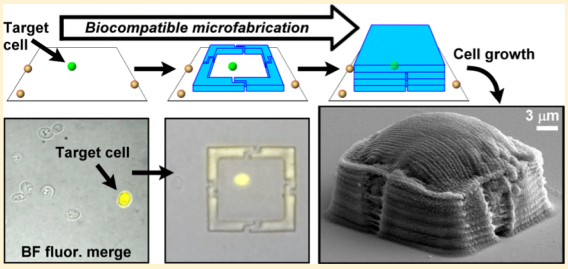

The development of microfabrication and microfluidic technologies for biological studies has enabled cell and microorganismal behavior to be examined with increasingly high precision.[1] The use of microfabricated landscapes,[2] microfluidic circuits,[3] and droplet generators[4] have helped to shed new light on a diverse range of cell behaviors including microecological evolution/interactions,[5,6] biofilms,[7] chemotaxis,[8] rare and unculturable organisms,[9,10] and cellular communication.[8,11] In general, these studies are carried out within channels, chambers, and surfaces micropatterned from glass, cured resins (e.g, polydimethylsiloxane (PDMS)) or other plastics that contain and direct gas and liquids with limited diffusion across barrier walls. Other patterned materials derived from biological or synthetic hydrogels have been employed in microscale cell studies which can facilitate loading of cell suspensions and allow cells access to bath nutrients while restricting the physical growth or movement of cells and cell populations.[12−14]

Furthermore, we and others have recently shown that cellular microenvironments, channels, and chambers can be fabricated with arbitrary 3D forms from protein-based hydrogels[15−18] and with submicrometer feature sizes using multiphoton lithography (MPL), an intrinsically 3D laser direct-write technique. These materials show tunable swelling[19] and mechanical properties[20] and can allow ready diffusion of nutrients and wastes across microstructured barriers. Microchamber geometries that facilitate capture of motile bacterial cells have been employed to drive fluid flow,[17] investigate quorum sensing,[18] and measure cell/material interactions.[20]

However, all of the above examples rely on essentially stochastic interactions with cells, whether in fluidic droplets,[4,11] or "lobster trap" geometries[17,18] for capture and confinement in low dimensional volumes. This severely limits our ability to isolate a single targeted cell of choice, which would prove useful for studying particularly challenging problems, for instance, phenotypic diversity of clonal populations or analysis of rare/unculturable microorganisms. In such cases, it would be desirable to be able to identify and select a target cell from a mixed population based on phenotypic or other criteria and confine it in place under conditions that allow subsequent viability and potential clonal expansion. Here we report a procedure that addresses these criteria and demonstrates, under conditions that can maintain cell viability, precise physical confinement of target cells and their progeny within 3D hydrogel microchambers.

EXPERIMENTAL SECTION

Fabrication of Protein Microstructures. Microchambers composed of photocross-linked protein were fabricated in the presence of living cells from overnight to 3 day old cultures that were resuspended in PBS (pH 7.4) solutions containing BSA protein at 280 mg/mL and methylene blue (6 mM) as a photosensitizer. Microstructure geometries were fabricated onto untreated coverslips around selected target cells using a dynamic mask-directed multiphoton lithography technique previously described in detail.[16] Briefly, the output of a mode-locked titanium:sapphire laser (Tsunami, Spectra Physics, Mountain View, CA) centered at 750 nm, pulse width of 60 fs, and a repetition rate of 80 MHz, was raster scanned with an *X*/*Y* open frame scan head (Nutfield

Received: July 2, 2012
Accepted: October 16, 2012

   dx.doi.org/10.1021/ac301816c | *Anal. Chem.* XXXX, XXX, XXX−XXX

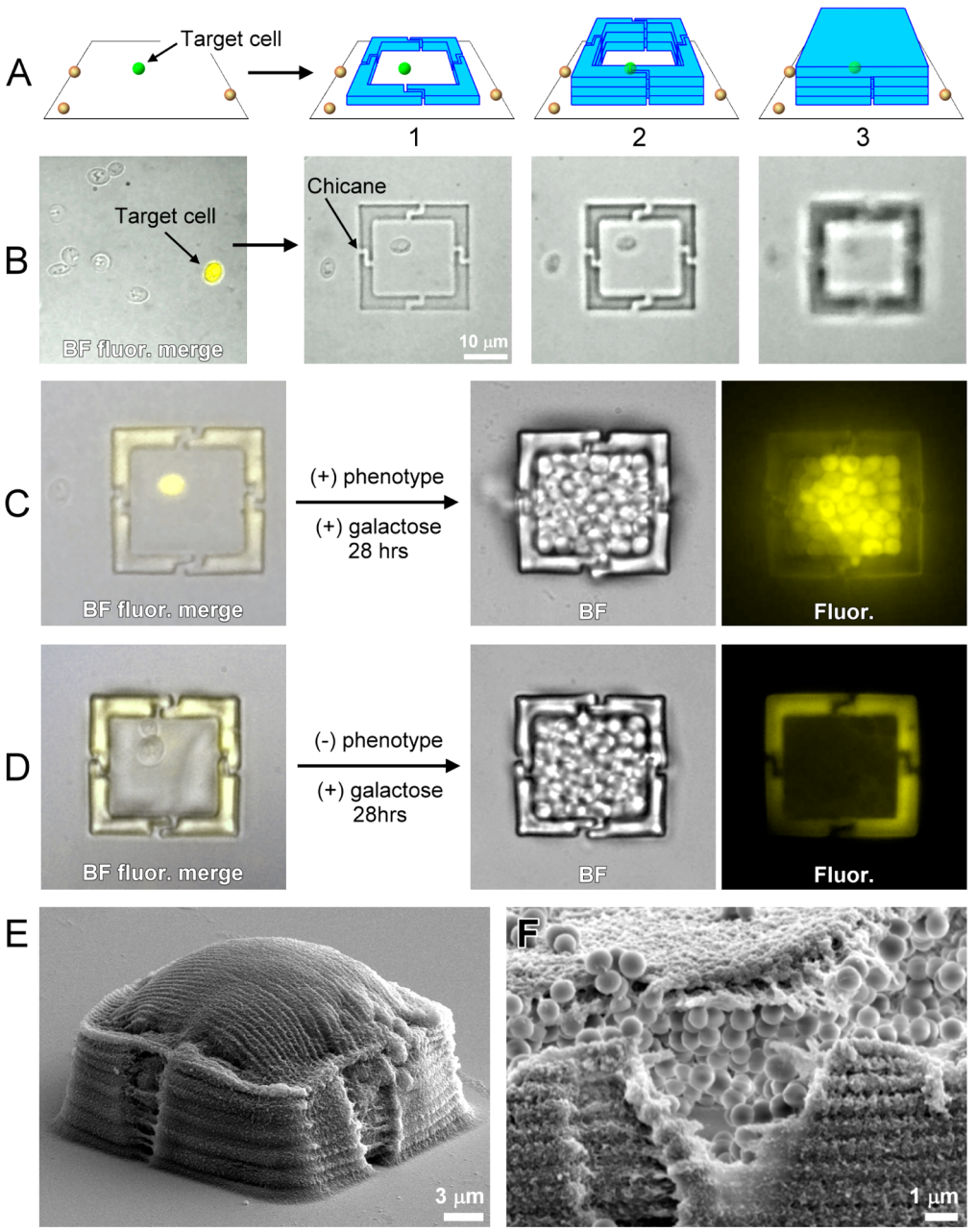

Figure 1. Targeted confinement of living cells and their progeny via biocompatible *in situ* microfabrication of 3D protein microchambers. (A) Simplified schematic of protein microchamber fabrication isolating a target cell. (B) Microscopy images of the isolation of a single *S. cerevisiae* cell expressing YFP from a population of nonexpressing *S. cerevisiae* cells within a BSA protein microstructure, following the panels shown in part A. (C) Targeted confinement of a *S. cerevisiae* cell initially expressing YFP, followed by growth and YFP expression upon incubation in medium with inducer (YP + gal). (D) Targeted confinement of non-YFP expressing mother and daughter cells, followed by growth in YP + gal medium showed no detectible YFP signal. (E) SEM image of a protein structure containing a high-density *S. cerevisiae* cell population. The pressure exerted by the dividing cells resulted in protrusion of the roof into a dome shape. Overall chamber dimensions: 25 μm × 25 μm in length and width; 10−12 μm in height. (F) SEM image of a protein structure with roof retracted revealing interior containing a high-density *S. aureus* cell population.

Technology, Hudson, NH) across a digital micromirror device (used as a digital photomask to define features of microstructures) and subsequently aligned into a microscope objective (Nikon 100× Fluar, 1.3 numerical aperture) situated on a Nikon inverted microscope. This output defined the features of microstructures in the X/Y plane. Figure S-1 in the Supporting Information shows the digital image used for the containment microchambers shown in Figure 1B,C and Supporting Movie S-1 in the Supporting Information. Stepping the laser focus axially from the substrate using a piezo Z-stage (Mad City Laboratories) while changing the image on the DMD reflectance mask permitted fabrication of 3D microstructures. Ti:S are considered Class 4 lasers and thus proper laser safety to minimize exposure to open beams, particularly use of appropriate eyewear, should be observed during operation.

Materials, Cell Strains and Incubation, and Optical and Electron Microscopy. See the Supporting Information text for details.

dx.doi.org/10.1021/ac301816c | *Anal. Chem.* XXXX, XXX, XXX−XXX

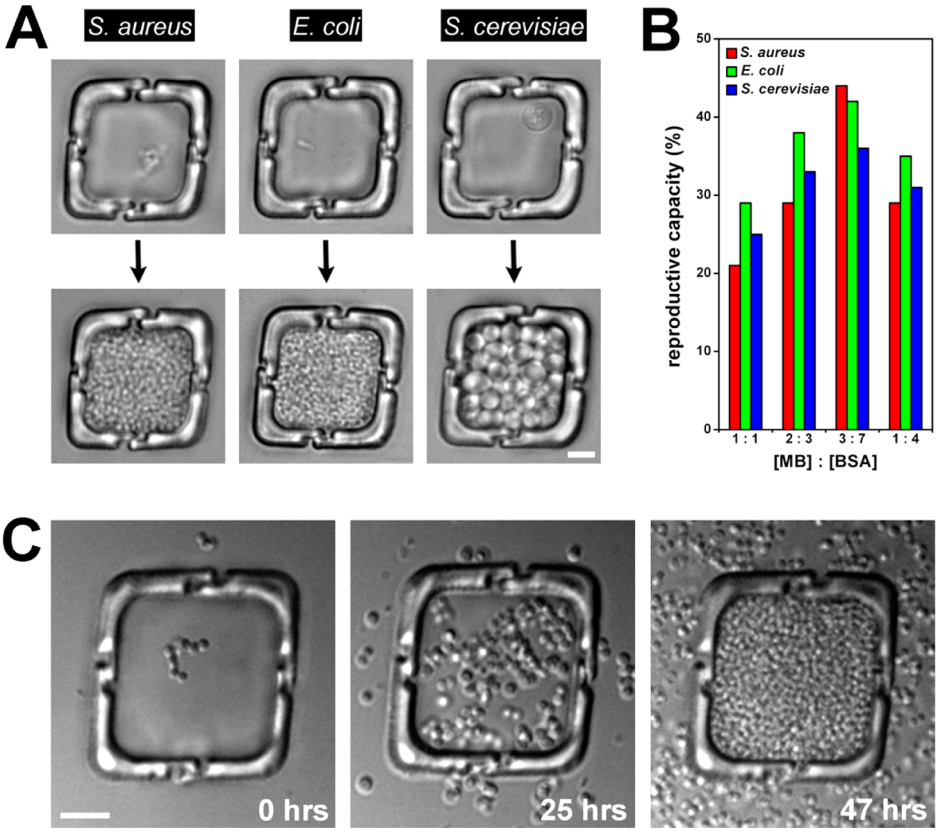

Figure 2. Targeted confinement of three classes of microorganisms. (A) Gram-positive (*S. aureus*), gram-negative (*E. coli*), and eukaryotic (*S. cerevisiae*) resulted in formation of dense colonies. (B) Reproductive capacity as a function of the ratio of MB/BSA (defined as the fraction of 20 mM MB mixed with 400 mg/mL BSA in PBS) for all three microorganisms. Values represent total number of chambers with dense growth divided by the total chambers fabricated under a particular condition (between 7 and 24 chambers per data point). (C) Time-lapse showing growth of a confined *S. aureus* colony into an ultrahigh density population. Scale bars for A and C are 5 μm.

RESULTS AND DISCUSSION

To fabricate microchambers around cells, we employed multiphoton lithography (MPL), a 3D laser direct write micro/nano fabrication procedure. Fabrication in the presence of cells is facilitated using aqueous biocompatible precursor solutions containing, for instance, biological "monomers" such as proteins that can be photochemically cross-linked to form solidified protein hydrogel structures.[20,21] Photocross-linking occurs via photoexcitation of a sensitizer to generate reactive intermediates that activate oxidizable residues (e.g., Tyr-radicals) to produce interprotein cross-links.[22,23] Using MPL confines this photochemical process to a 3D region (voxel) proximal to the focal point of a focused light source, generally a high frequency, short-pulse laser such as a titanium sapphire (Ti:S). Translation of this voxel within a protein solution allows fabrication of 3D micro to nanoscale objects with nearly arbitrary features.[15,16] Using this technique, efforts to fabricate simple 2D line structures in the presence of cells have been explored.[21,24] We wished to investigate conditions for biocompatible MPL (bio-MPL) of truly 3D microcontainers in an effort to three-dimensionally confine targeted cells while maintaining their viability and reproductive capacity.

To these ends, we prepared a precursor solution comprised of bovine serum albumin (BSA) as protein monomer and methylene blue (MB) as photosensitizer dissolved in PBS. MB has been used in cell culture as a viability indicator measuring cellular redox activity as well as a redox mediator for monitoring culture respiration rate[25,26] and provides efficient photosensitization for MPL protein cross-linking.[15,19,27] To test cell tolerance to these constituents, we incubated yeast (*S. cerevisiae*) and bacterial cells (*S. aureus* and *E. coli*) in precursor solutions containing BSA (200 mg/mL) and a range of concentrations of MB. We observed all cells maintained >80% viability following 1 h at the highest concentration of MB tested (10 mM, see the Supporting Information, Figure S-2).

To demonstrate targeted cell confinement, we interrogated cells derived from a single (plate) colony of *S. cerevisiae* S288C containing an inducible plasmid (yellow fluorescent protein; YFP) as shown in Figure 1. Growth of this colony under constant, nonselective pressure conditions (see the Supporting Information) resulted in heterogeneous expression of YFP, a widely observed phenomenon attributable to a range of factors[28−32] (e.g., genetic noise, unequal segregation of cellular components during cell division). First, these cells were rinsed in PBS and subsequently deposited in a well with a glass coverslip substrate. The bath solution was replaced with the BSA fabrication solution, and a YFP-expressing yeast cell [(+) phenotype)] among nonexpressing [(−) phenotype] neighbor cells was identified via fluorescence using an inverted microscope (Figure 1A,B). Next, the microscope stage and focus were adjusted to ensure the cell was positioned at the desired location prior to confinement. Photofabrication commenced from the substrate to form the containment walls, and the stage was stepped vertically to a final height of ~8−10 μm. At this point, a ~2 μm thick top layer was fabricated by spanning a solid rectangular section across the

dx.doi.org/10.1021/ac301816c | *Anal. Chem.* XXXX, XXX, XXX−XXX

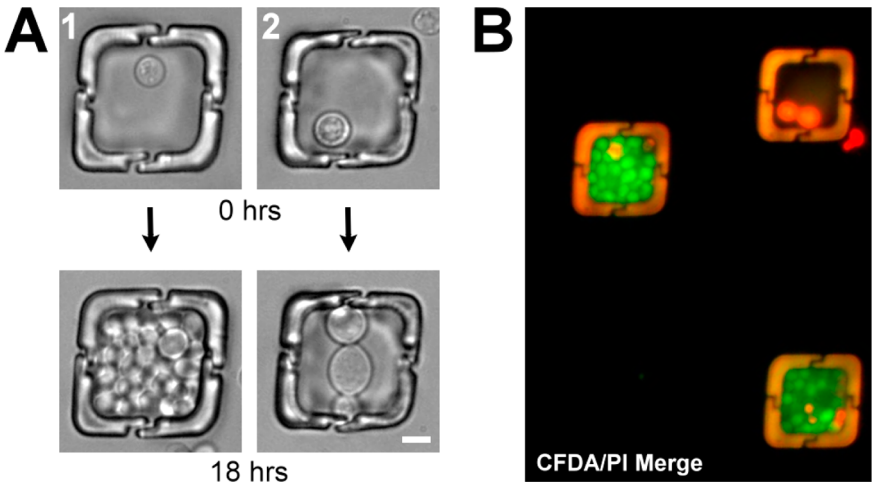

Figure 3. Targeted confinement of *S. cerevisiae* that vary in initial cell size. (A) Single *S. cerevisiae* cells isolated from the same clonal culture grow to dense populations (panel 1) or divide only 1−4 times while swelling in diameter (panel 2). Both behaviors were routinely observed during experiments using cells derived from single clones and exhibit different responses to CFDA/PI viability dye (panel B: green = viable, red = apoptotic). Scale bar for A is 5 μm.

tops of the walls, thereby sealing the container. The digital masks used for the chamber walls and ceiling are shown in Figure S-1 in the Supporting Information. The microscope imagining objective serves as the tight-focusing optic (NA = 1.3) for the Ti:S laser enabling the process to be visually monitored over the course of minutes. The entire microfabrication procedure, from cell identification to container sealing, is shown in Supporting Movie S-1 in the Supporting Information.

After the cell was confined, the well was rinsed with PBS followed by incubation in YFP-inducing media (YP + 2% galactose; YP + gal) at 30 °C. Chicane-shaped features were incorporated in the chamber walls to allow unrestricted diffusion of bath (nutrient) solutions while maintaining a physical barrier between internal and external cells. The isolated cell proliferated into an extremely dense population (~80 cells in ~3.5 pL chamber, ~2.5×10^{10} cells/mL) within the protein microchamber over 28 h (Figure 1C). Under conditions of galactose metabolism, S288C cells are engineered to express YFP. As shown in Figure 1C, the majority of the cell's progeny exhibit YFP expression. Isolation of a (−) phenotype mother and daughter cell (Figure 1D) derived from a YFP expressing colony followed by incubation in YP + gal at 30 °C for 28 h also resulted in a high-density confined population that, as expected, exhibited no YFP fluorescence in the presence of galactose due to the loss of the plasmid.

A scanning electron microscopy (SEM) image of a protein microchamber packed with *S. cerevisiae* cells is shown in Figure 1E. Ridges parallel to the substrate in the structure walls are associated with the individual fabrication planes as the stage is stepped vertically from the substrate. Here, growth of the entrapped cells has swelled the top of the chamber into a dome shape (Figure 1E), illustrating the swelling properties of these MPL protein hydrogels as we have described previously.[19,20] Shown in Figure 1F is a similar dome shaped chamber due to growth of entrapped *S. aureus* cells. This procedure was applied successfully to eukaryotic, gram negative, and gram positive microorganisms (Figure 2A), and the potential phototoxicity of MB[33] was, in part, mitigated by optimizing the ratio of constituents for greatest cell reproductive capacity following photofabrication. Using 280 mg/mL BSA, 6 mM MB in PBS, pH ~7.5 for the fabrication solution, we observed that greater than $^1/_3$ of confined cells subsequently proliferate into dense colonies (Figure 2B), which may be improved upon by exploring other schemes and materials such as those to generate cell-laden hydrogels.[34] However, we note that a comparable study employing bacterial cell confinement in microfluidic droplets reported as few as 1 in 7 confined cells were able to subsequently proliferate.[11] Importantly, biocompatible MPL (bio-MPL) allows for cell proliferation into ultrahigh density populations (~10^{12} *S. aureus* cells/mL, Figure 2C) that remain accessible to the bath solution and further chemical interrogation (Figure S-3 in the Supporting Information).

The ability to identify and precisely confine cells of interest in mixed populations and within user-defined structures fabricated from robust and "breathable" hydrogels provides new avenues to study cellular behavior across generations. For example, budding yeast such as *S. cerevisiae* are invaluable model organisms for the study of eukaryotic cell processes such as clonal heterogeneity and aging. However, studies that require abilities to separate cells based on phenotype, for instance, to study cell aging have relied on laborious manual manipulation/dissection[35,36] with a recent noteworthy exception.[37] Bio-MPL can greatly facilitate cell isolation based on phenotypic markers such as cell size, while maintaining microscope observation throughout an experiment. As an example, Figure 3A illustrates two distinct fates of confined yeast cells. In one case, isolation of a single cell led to unchecked proliferation, eventually filling the microchamber (Figure 3A, panel 1). However, confinement of a slightly larger cell (a relative measure of cell age[37]) resulted in only 3 cell divisions, accompanied by a substantial increase in cell size (diameters 7−10 μm, Figure 3A, panel 2). Viability dye assays showed that the majority of cells that divide into dense populations remained viable, while the larger yeast cells displayed hallmarks of apoptosis (Figure 3B); these observations are consistent with age differences of the initial confined cells; young cells can quickly reproduce in the presence of nutrients while older cells display a limited number of divisions before apoptosis and give rise to daughter cells with short lifespans.[37]

Thus, despite recent progress in microfluidic platforms for yeast studies,[37,38] bio-MPL has the singular ability for the

dx.doi.org/10.1021/ac301816c | *Anal. Chem.* XXXX, XXX, XXX−XXX

investigator to directly select the cell and define a containment architecture within a mixed population, which should enable studies regarding population heterogeneity[30,32] using yeast as model organisms.[28,29,31]

CONCLUSIONS

We have described a bio-MPL technique for 3D confinement of targeted cells and their progeny. In contrast to existing methods that rely on stochastic interactions to confine cells, this capability provides a new platform by which to interrogate a wide-range of cellular processes using selected, single cells as the starting point. The chemical and mechanical properties of microfabricated protein hydrogels are readily tunable[19,20] offering unprecedented abilities to direct cell proliferation using responsive and "deformable" structures (e.g., Figure 1D). Bio-MPL cell confinement combined with the concurrent fabrication of environmental cell traps based on cell motility[17] should allow interactions of competing/cooperating organisms to be precisely orchestrated, providing a powerful tool to begin to tease apart complex sociobiological behaviors that underlie, for instance, bacterial virulence and antibiotic resistance.

ASSOCIATED CONTENT

Supporting Information

Detailed materials and methods, supporting movie showing isolation of a single *S. cerevisiae* cell expressing YFP from a population of nonexpressing cells, optimization of MPL conditions for living cell isolation, and additional data described in the text. This material is available free of charge via the Internet at http://pubs.acs.org.

AUTHOR INFORMATION

Corresponding Author

*E-mail: bjkaehr@sandia.gov. Fax: 505-272-7336.

Notes

The authors declare no competing financial interest.

ACKNOWLEDGMENTS

We acknowledge support from U.S. Department of Energy (DOE), Office of Science, Office of Basic Energy Sciences (BES), Division of Materials Sciences and Engineering. J.C.H gratefully acknowledges funding by the Defense Treat Reduction Agency (DTRA) Chem. Bio. Basic Research Program Grants B084467I, B0947321I, and B0114453I. Sandia National Laboratories is a multiprogram laboratory managed and operated by Sandia Corporation, a wholly owned subsidiary of Lockheed Martin Corporation, for the U.S. Department of Energy's National Nuclear Security Administration under Contract DE-AC04-94AL85000.

REFERENCES

(1) Weibel, D. B.; Diluzio, W. R.; Whitesides, G. M. *Nat. Rev. Microbiol.* **2007**, *5*, 209−218.
(2) Keymer, J. E.; Galajda, P.; Muldoon, C.; Park, S.; Austin, R. H. *Proc. Natl. Acad. Sci. U.S.A* **2006**, *103*, 17290−17295.
(3) Thorsen, T.; Maerkl, S. J.; Quake, S. R. *Science* **2002**, *298*, 580−584.
(4) Pompano, R. R.; Liu, W. S.; Du, W. B.; Ismagilov, R. F. *Annu. Rev. Anal. Chem.* **2011**, *4*, 59−81.
(5) Kim, H. J.; Boedicker, J. Q.; Choi, J. W.; Ismagilov, R. F. *Proc. Natl. Acad. Sci. U.S.A* **2008**, *105*, 18188−18193.
(6) Zhang, Q. C.; Lambert, G.; Liao, D.; Kim, H.; Robin, K.; Tung, C. K.; Pourmand, N.; Austin, R. H. *Science* **2011**, *333*, 1764−1767.
(7) Eun, Y. J.; Weibel, D. B. *Langmuir* **2009**, *25*, 4643−4654.
(8) Park, S.; Wolanin, P. M.; Yuzbashyan, E. A.; Silberzan, P.; Stock, J. B.; Austin, R. H. *Science* **2003**, *301*, 188−188.
(9) Marcy, Y.; Ouverney, C.; Bik, E. M.; Losekann, T.; Ivanova, N.; Martin, H. G.; Szeto, E.; Platt, D.; Hugenholtz, P.; Relman, D. A.; Quake, S. R. *Proc. Natl. Acad. Sci. U.S.A* **2007**, *104*, 11889−11894.
(10) Liu, W. S.; Kim, H. J.; Lucchetta, E. M.; Du, W. B.; Ismagilov, R. F. *Lab Chip* **2009**, *9*, 2153−2162.
(11) Boedicker, J. Q.; Vincent, M. E.; Ismagilov, R. F. *Angew. Chem., Int. Ed.* **2009**, *48*, 5908−5911.
(12) Tuson, H. H.; Renner, L. D.; Weibel, D. B. *Chem. Commun.* **2012**, *48*, 1595−1597.
(13) Takeuchi, S.; DiLuzio, W. R.; Weibel, D. B.; Whitesides, G. M. *Nano Lett.* **2005**, *5*, 1819−1823.
(14) Moffitt, J. R.; Lee, J. B.; Cluzel, P. *Lab Chip* **2012**, *12*, 1487−1494.
(15) Kaehr, B.; Shear, J. *J. Am. Chem. Soc.* **2007**, *129*, 1904−1905.
(16) Nielson, R.; Kaehr, B.; Shear, J. *Small* **2009**, *5*, 120.
(17) Kaehr, B.; Shear, J. B. *Lab Chip* **2009**, *9*, 2632−2637.
(18) Connell, J. L.; Wessel, A. K.; Parsek, M. R.; Ellington, A. D.; Whiteley, M.; Shear, J. B. *mBio* **2010**, *1*, No. e00202-10.
(19) Kaehr, B.; Shear, J. *Proc. Natl. Acad. Sci. U.S.A* **2008**, *105*, 8850.
(20) Khripin, C.; Brinker, C.; Kaehr, B. *Soft Matter* **2010**, *6*, 2842−2848.
(21) Kaehr, B.; Allen, R.; Javier, D. J.; Currie, J.; Shear, J. B. *Proc. Natl. Acad. Sci. U.S.A* **2004**, *101*, 16104−16108.
(22) Shen, H. R.; Spikes, J. D.; Smith, C. J.; Kopecek, J. *J. Photochem. Photobiol. A* **2000**, *133*, 115−122.
(23) Spikes, J. D.; Shen, H. R.; Kopeckova, P.; Kopecek, J. *Photochem. Photobiol.* **1999**, *70*, 130−137.
(24) Kaehr, B.; Ertas, N.; Nielson, R.; Allen, R.; Hill, R. T.; Plenert, M.; Shear, J. B. *Anal. Chem.* **2006**, *78*, 3198−3202.
(25) Ganguli, R.; Dunn, B. S. *Fuel Cells* **2009**, *9*, 44−52.
(26) Karakashev, D.; Galabova, D.; Simeonov, I. *World J. Microb. Biotechnol.* **2003**, *19*, 233−238.
(27) Sun, Y. L.; Dong, W. F.; Yang, R. Z.; Meng, X.; Zhang, L.; Chen, Q. D.; Sun, H. B. *Angew. Chem., Int. Ed* **2012**, *51*, 1558−1562.
(28) Levy, S. F.; Ziv, N.; Siegal, M. L. *PLoS Biol.* **2012**, *10*, e1001325.
(29) Newman, J. R.; Ghaemmaghami, S.; Ihmels, J.; Breslow, D. K.; Noble, M.; DeRisi, J. L.; Weissman, J. S. *Nature* **2006**, *441*, 840−846.
(30) Avery, S. V. *Nat. Rev. Microbiol.* **2006**, *4*, 577−587.
(31) Raser, J. M.; O'Shea, E. K. *Science* **2004**, *304*, 1811−1814.
(32) McAdams, H. H.; Arkin, A. *Trends Genet.* **1999**, *15*, 65−69.
(33) Chen, J.; Cesario, T. C.; Rentzepis, P. M. *J. Phys. Chem. A* **2011**, *115*, 2702−2707.
(34) Panda, P.; Ali, S.; Lo, E.; Chung, B. G.; Hatton, T. A.; Khademhosseini, A.; Doyle, P. S. *Lab Chip* **2008**, *8*, 1056−1061.
(35) Steffen, K. K.; Kennedy, B. K.; Kaeberlein, M. *J. Vis. Exp.* **2009**, *28*, No. e1209.
(36) Mortimer, R. K.; Johnston, J. R. *Nature* **1959**, *183*, 1751−1752.
(37) Lee, S. S.; Vizcarra, I. A.; Huberts, D. H. E. W.; Lee, L. P.; Heinemann, M. *Proc. Natl. Acad. Sci. U.S.A* **2012**, *109*, 4916−4920.
(38) Falconnet, D.; Niemisto, A.; Taylor, R. J.; Ricicova, M.; Galitski, T.; Shmulevich, I.; Hansen, C. L. *Lab Chip* **2011**, *11*, 466−473.